

Implementation of pulse fitting cosmic signals to calibrate the HPS ECal

Luca Marsicano^{*1} and Holly Szumila-Vance^{†2}

¹Instituto Nazionale di Fisica Nucleare, Sezione di Genova, Genova, Italy

²Old Dominion University, Norfolk, VA

Abstract

The electromagnetic calorimeter (ECal) of the Heavy Photon Search (HPS) experiment is sensitive to measuring signals from cosmic ray muons. The use of cosmic ray muons to calibrate the ECal is critical in establishing baseline gains prior to receiving beam, calibrating edge crystals, and calibrating those crystals not in the acceptance for elastically-scattered electrons. This note describes an improved procedure that can calibrate the ECal by pulse-fitting the raw FADC cosmic signal waveform requiring less time to collect cosmic ray signals than in previous procedures. Additionally, this note provides details on the software package needed to complete the calibration.

1 Introduction

The HPS ECal consists of 442 PbWO_4 scintillating crystals from the former CLAS Inner Calorimeter in Hall B at Jefferson Lab. In an upgrade, prior to HPS experimental running, the crystals were re-fitted with large area avalanche photo-diodes ($10 \times 10 \text{ mm}^2$) that increased the sensitivity of the detector to smaller signals. The full detector read out is described in detail in [1]. Prior to 2016 experimental running, the signals from the ECal were split between the FADC250s and the TDCs to allow for the full commissioning of the new FADC250s. After the Engineering Run in 2015, the splitter was removed so that 100% of the signal coming from the ECal was going to the FADC250 due to their demonstrated reliability. The FADC250s were run in full waveform readout so that the signals could be examined and analyzed offline. Prior to running the ECal with the electron beam, the full detector was able to be calibrated using signals from passing cosmic ray muons. These signals were detectable by the ECal due to the upgraded electronics using the large area avalanche photo-diodes. The experimental setup for triggering and reading out cosmic signals in the ECal is shown in Figure 1.

The previously used method of calibrating the ECal using cosmic signals is described in [2]. An overview is described here. After a cosmic signal is measured from the coincidence of the two triggering scintillators external to the ECal, all 442 modules were read out by the DAQ. The general trigger rate measured at the DAQ was approximately 7 Hz. Offline, a geometric selection of cuts was applied to the data to identify cosmic signals that could be used for calibration. The module of interest was first identified with a threshold crossing in the raw waveform spectra. The cuts required that no threshold crossing in the raw waveform occurred in crystals immediately adjacent in the same row. Further cuts required that adjacent crystals vertically had to have also measured a threshold crossing. If this criteria was met, then the information for that crystal was

^{*}luca.marsicano@ge.infn.it

[†]hszumila@jlab.org

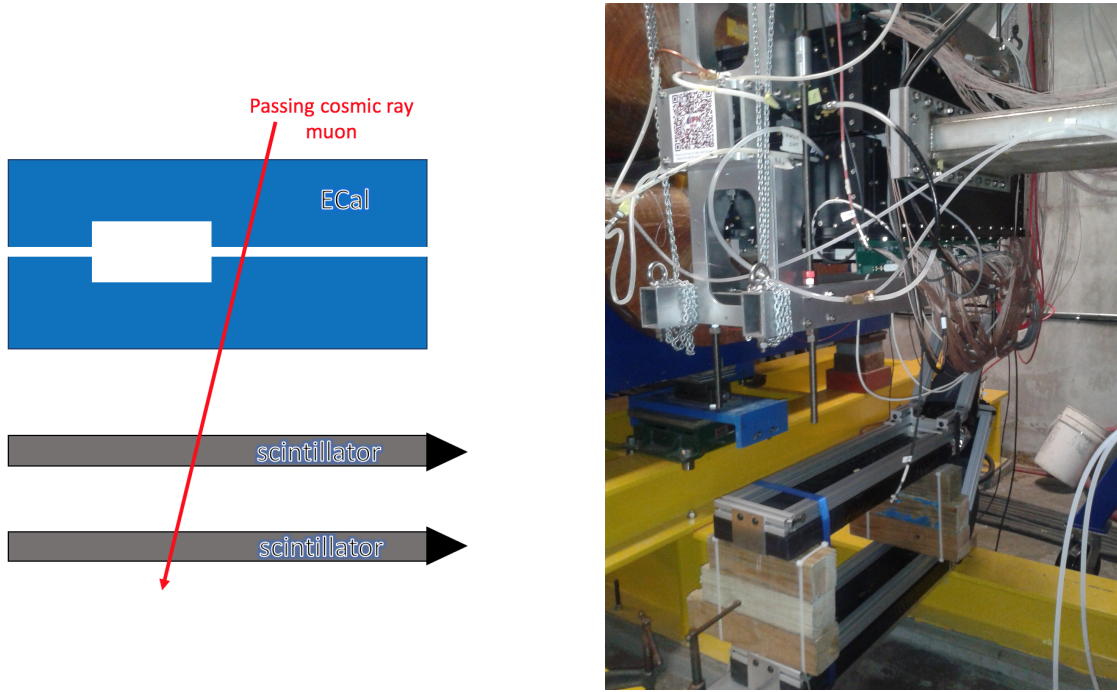


Figure 1: A schematic showing the ECal (viewed from downstream) is shown on the left. A cosmic event is triggered when a cosmic ray muon passes vertically through the detector and is detected by both scintillators, located below. The actual installed set up is shown with a similar view from downstream on the right.

kept for the calibration.

The calibration procedure selected a window prior to the signal window in the raw FADC wave spectrum to calculate an average event-by-event pedestal for a particular channel. The integral was extracted by summing the raw waveform spectrum in the signal window and subtracting the corresponding pedestal. This pulse-integral was recorded over many events and fit with a Landau-Gaussian convolution. The peak of the fit was obtained numerically and corresponded to the FADC calibration point. The procedure described above will differ from that described by this note. The acquisition of the data will be the same, but the cuts and fits to extract the gain for each module will be different and described in detail.

2 Method

The calibration procedure that follows was tuned and developed on the cosmic ray data obtained after the removal of the splitters from the readout chain in 2016. The signal amplitudes in the raw FADC waveform were visually larger than those seen when taken with the splitters. Some time was spent in determining an adequate threshold for a clear minimum ionization peak in the data and keeping good events. With minimal cuts, a cosmic ray passing vertically through the ECal produces some signal in all ten layers as shown in Figure 2.

In order to use the relatively small signals from cosmic rays in the ECal, cuts are applied to isolate the peak. The goal of the cuts is to ensure that the signal is from a cosmic ray muon (as opposed to a fluctuation in the FADC channel spectra) and that the hit passes cleanly through the crystal of interest such that the energy is not shared between crystals in the same row. From Figure 2, it is

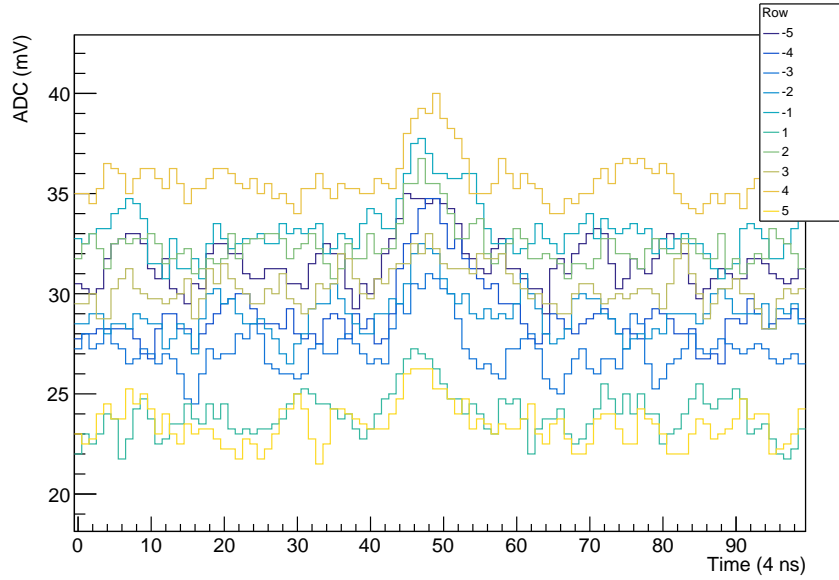


Figure 2: Cosmic ray signal as seen when passing vertically through a column of ten crystals in the ECal.

clear that the signals are very close to the pedestal, but a threshold can be chosen from this raw spectrum to identify when a signal is visible in a crystal. With the splitters installed in the HPS detector setup, this threshold was 2.5 FADC mV. After removal of the splitters, the threshold was increased to 3.5 FADC mV.

The threshold was used when applying geometric cuts to ensure that the cosmic ray muon passed vertically through the ECal. The geometric cuts were optimized from Monte Carlo to ensure that the signal is clearly visible in the crystal of interest. The analysis seeks crystals that have a threshold crossing in the optimal time window as prescribed from the DAQ. If there is a threshold crossing, then a threshold crossing is also required in the crystals immediately above and below the crystal of interest. A threshold crossing must not exist in the crystals to the immediate left and right of the crystal of interest in the same row. For edge crystals, the requirement to have a hit immediately above or below is altered such that the two subsequent crystals in the same column away from the edge have a hit above threshold.

From previous work [3], the ECal response is described by the sum of the pedestal and a 3-pole function:

$$P + \frac{A}{2\tau^3} (t - t_0)^2 e^{-(t-t_0)/\tau} \quad (1)$$

This function was further studied and implemented into the HPS calorimeter reconstruction software as described by [4]. Previously, the cosmic signals were integrated from the raw FADC spectra and not from a fit to the raw FADC spectra. Here, Equation (1) is applied to the cosmic signals as shown in Figure 3. The pedestals, P , for each fit are averaged over the bins at the front of the FADC timing window for each event. The widths, τ , for each each fit are fixed from those previously found by [4]. The t_0 is initialized from the bin time at threshold crossing. The integral A is initialized to the area of the peak, evaluated summing the FADC samples in the signal region.

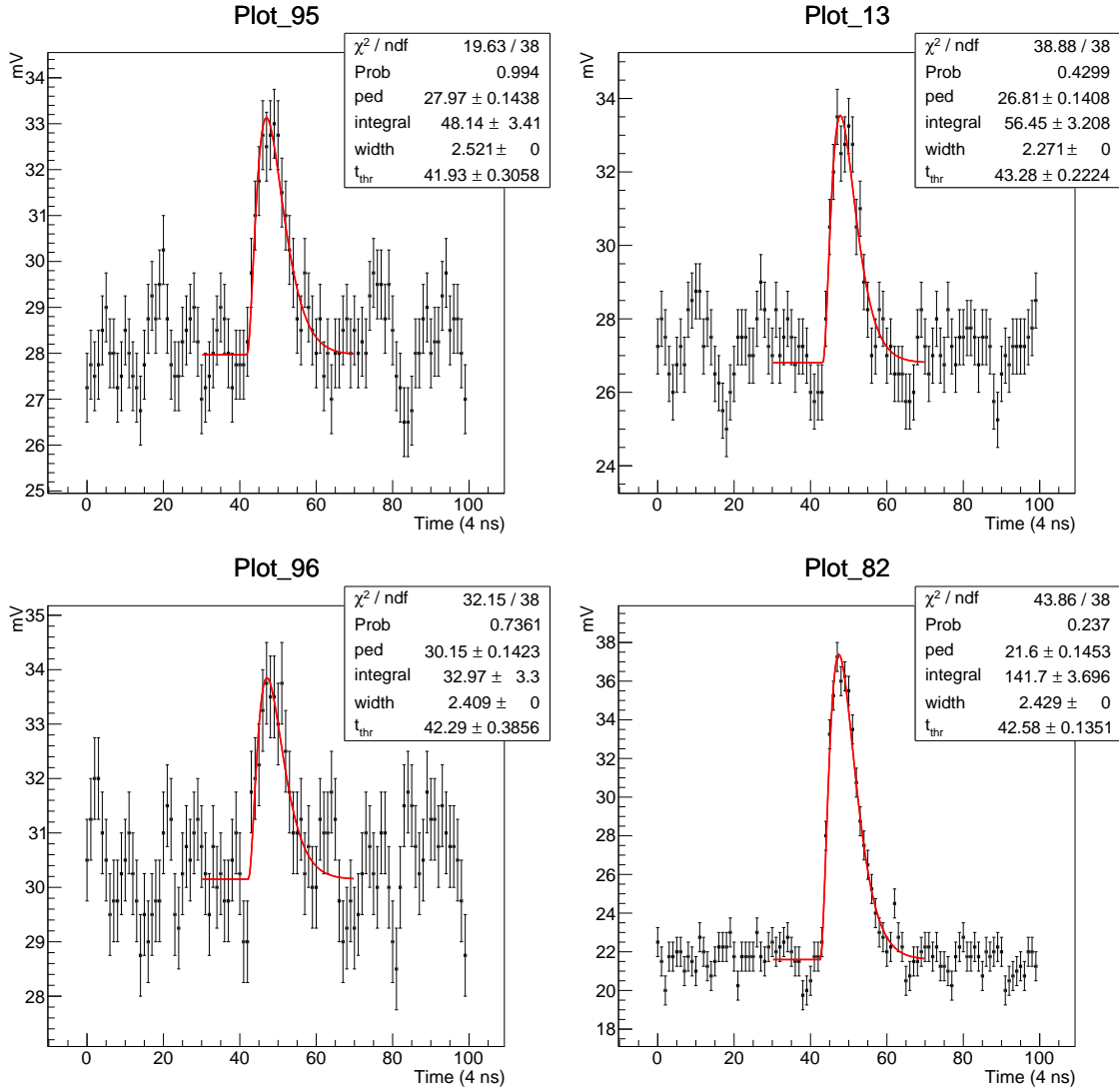


Figure 3: Fits applied to cosmic ray signals in four different crystals using Equation (1). The noise errors shown here are estimated to be 0.75 FADC mV per time bin.

After applying the pulse-fitting procedure to the raw FADC spectra for each crystal, the peak position of the distribution of the pulse-integral per crystal is used to calibrate the gain. The pulse-integral distribution for a single crystal is shown in Figure 4. The fit applied to Figure 4 is a Landau-Gaussian convolution where the Landau part arises from the scintillation response in the crystal, and the Gaussian component comes from the statistical noise component of the electronics in readout. The overall gain is obtained from numerically determining the peak position as shown in Figure 4 and dividing into the expected energy deposition in the crystal as obtained from Monte Carlo. The formula is described by Equation (2).

$$\text{Gain} = \frac{\text{Energy MeV}}{\text{FADC pulse-integral}} \quad (2)$$

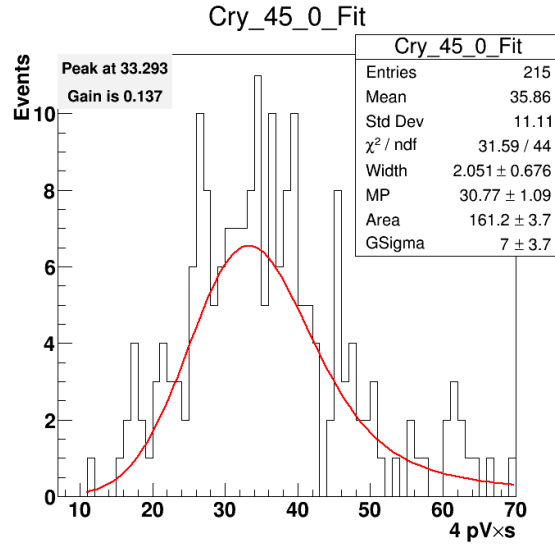


Figure 4: The pulse-integral distribution obtained from pulse-fitting applied to the raw FADC spectrum of each crystal is shown for a single crystal. The distribution is then fit with a Landau-Gaussian convolution, and the peak of this fit is obtained numerically to provide the calibration point.

3 Results

From the fits shown in Figure 3, the χ^2 distribution is shown in Figure 5. Here, the noise per bin is estimated to be 0.75 FADC mV. The resulting χ^2 from these fits appears to be reasonable and is slightly worse than the quality described by [4]. The decrease in fit quality is most likely due to the low energy of the signals when compared to the signals in [4]. We compare the fits to the pulse-

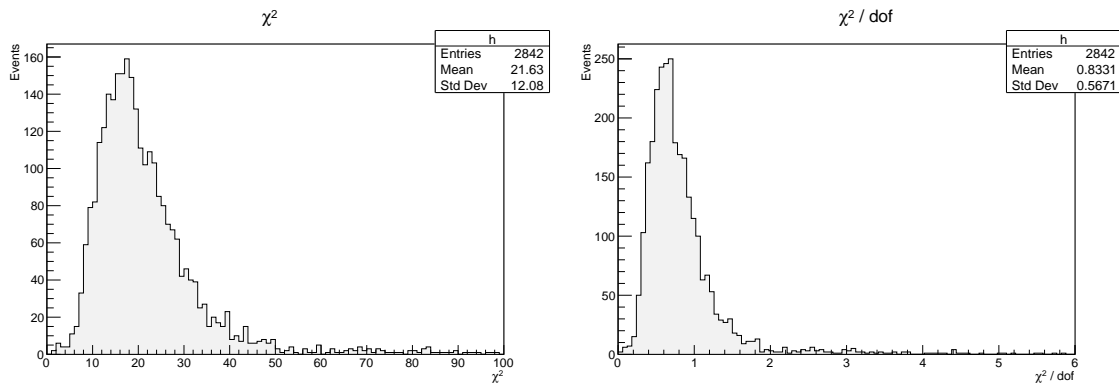


Figure 5: Shown on the left is the raw χ^2 distribution from the pulse-fits applied to cosmic ray signals in the ECal. The χ^2 / dof is shown on the right. The distribution on the right looks reasonable, but is slightly worse than the distribution obtained [4] due to the low energy of the signals.

integral distributions to understand the differences when obtaining the pulse-integral from the integral of the fit to the raw FADC spectra versus the integration of the raw FADC spectra without fitting. As shown in Figure 6 on the left, the resulting Gaussian widths are relatively unchanged for

the overall ECal response. This is not a truly accurate metric for comparison because the Gaussian widths are also strongly affected by the Landau part of the fit and this is mainly responsible for the outliers. However, it can be seen that there is generally no overall systematic difference or improvement. The peak of the pulse-integral distribution from pulse-fitting is shifted to larger values as shown in Figure 6 on the right. This larger value probably results from the visible dips in the FADC spectra that can be seen in Figure 3. These dips would not significantly affect the integral of the distribution when fitting as they would when integrating the raw FADC spectrum. While no clear improvement is achieved for the overall ECal using pulse-fitting, crystals that had

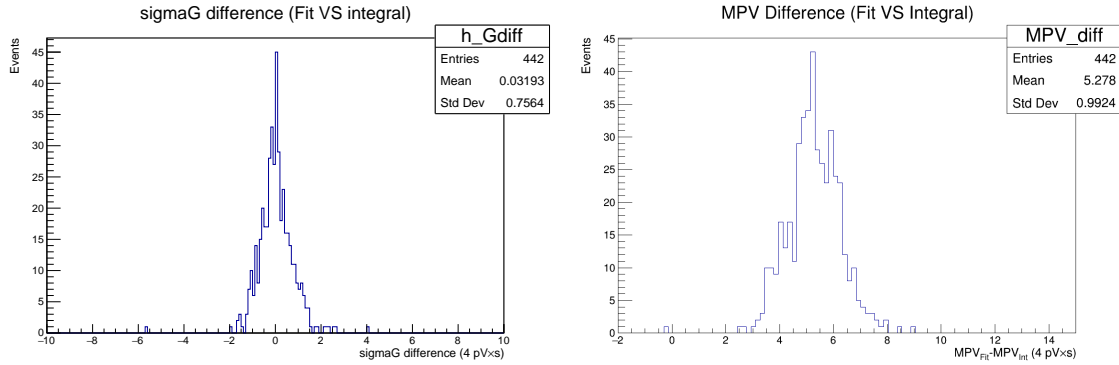


Figure 6: A comparison of the Gaussian σ from the convolution fit to the distribution of the pulse-integrals is compared for the pulse-integrals obtained from fitting and non-fitting procedures on the left. A comparison between the peak position from the distributions is shown on the right. While the resolution appears to be roughly the same, the peak position is systematically higher when the pulse-integral is obtained using pulse-fitting.

relatively noisy distributions tended to produce much cleaner distributions with pulse-fitting, as shown in Figure 7. A more typical improvement is shown in Figure 8.

From Monte Carlo simulation, the energy found to be deposited in the crystals using the prescribed geometric cuts was 16.7 MeV. After using this value for initial calibrations without pulse-fitting for the 2014 HPS run, the energy point was found to be too low when compared to the resulting peak position for elastically-scattered beam energy electrons. The energy for calibration point was increased to 18.3 MeV and appeared to provide a consistent calibration for all other energies as there was no longer a systematic offset with respect to the cosmic calibration. From this analysis, it is clear that pulse-fitting results in a systematically higher calibration point in cosmics. In order to establish gains that would be consistent with those seen from the elastically-scattered electron calibration from previous runs, the pulse-fitting cosmic calibration should use the previously found lower energy of 16.7 MeV for the gains.

4 Conclusion

The selection criteria for choosing crystals with good cosmic events is the same as determined previously and still requires a significant time collecting signals. While the overall trigger rate for signals is approximately 7 Hz from the DAQ, the rates per crystal after all cuts are applied are 3 mHz. In order to accomplish a confident calibration of the ECal, it is necessary to run for at least 24 hours. A good calibration using the ECal is important in establishing preliminary gains for use in the DAQ and is critical to the calibration of crystals that are not within the acceptance for

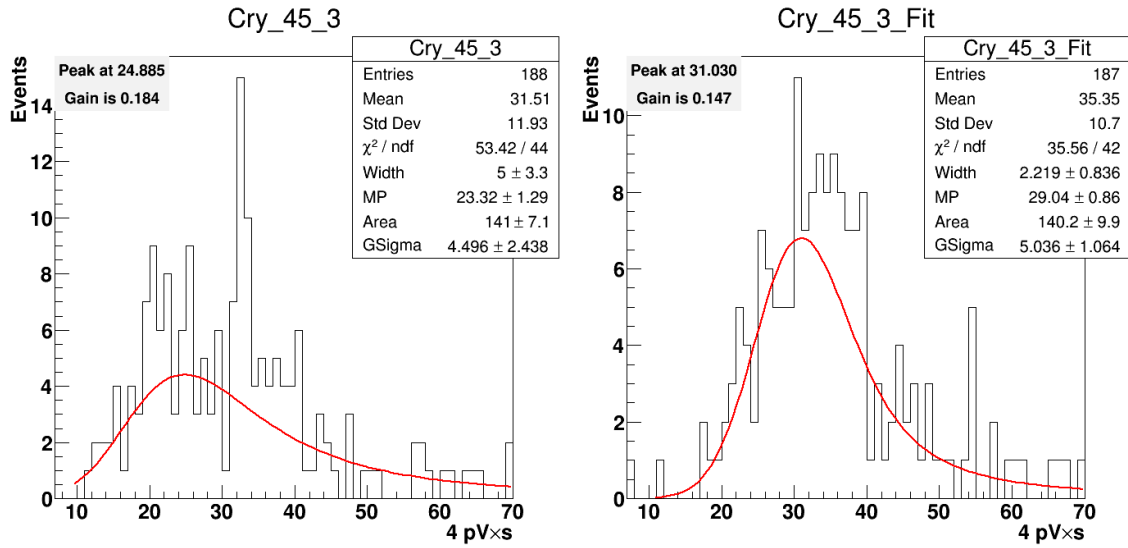


Figure 7: Shown on the left is the resulting pulse-integral distribution and fit for integration with no pulse-fitting. The right plot shows the resulting pulse-integral distribution for the same crystal whose pulse-integral was obtained with pulse-fitting. For this specific crystal, which is relatively noisy, the pulse-fitting produces a cleaner distribution.

elastically-scattered beam energy electrons. No improvement to the time spent collecting cosmic signals is found using this method.

The initialization of the fit parameters and the thresholds were thoroughly studied and discussed here. While pulse-fitting does not appear to improve the energy resolution of the ECal as a whole, there is improvement to some crystals that responded poorly when simply integrating the raw FADC spectrum. Pulse-fitting provides an improvement in the calibration of these crystals and is consistent with the HPS ECal reconstruction framework.

5 Software packages

The software is in the hps-java framework. Information for running the analysis can be found at <https://github.com/JeffersonLab/HPS-CODE/tree/master/CALIBRATION/COSMIC>.

References

- [1] Ilaria Balossino, Nathan Baltzell, Marco Battaglieri, Mariangela Bondi, Emma Buchanan, Daniela Calvo, Andrea Celentano, Gabriel Charles, Luca Colaneri, Annalisa D’Angelo, Marzio De Napoli, Raffaella De Vita, Raphael Dupre, Mathieu Ehrhart, Alessandra Filippi, Michel Garcon, Francois-Xavier Girod, Michel Guidal, Maurik Holtrop, Volodymyr Iurasov, Valery Kubarovsky, Kyle McCarty, Jeremy McCormick, Mikhail Osipenko, Rafayel Paremuzyan, Nunzio Randazzo, Emmanuel Raully, Benjamin Raydo, Emmanuel Rindel, Alessandro Rizzo, Philippe Rosier, Valeria Sipala, Stepan Stepanyan, Holly Szumila-Vance, and Lawrence Weinstein. The HPS electromagnetic calorimeter.

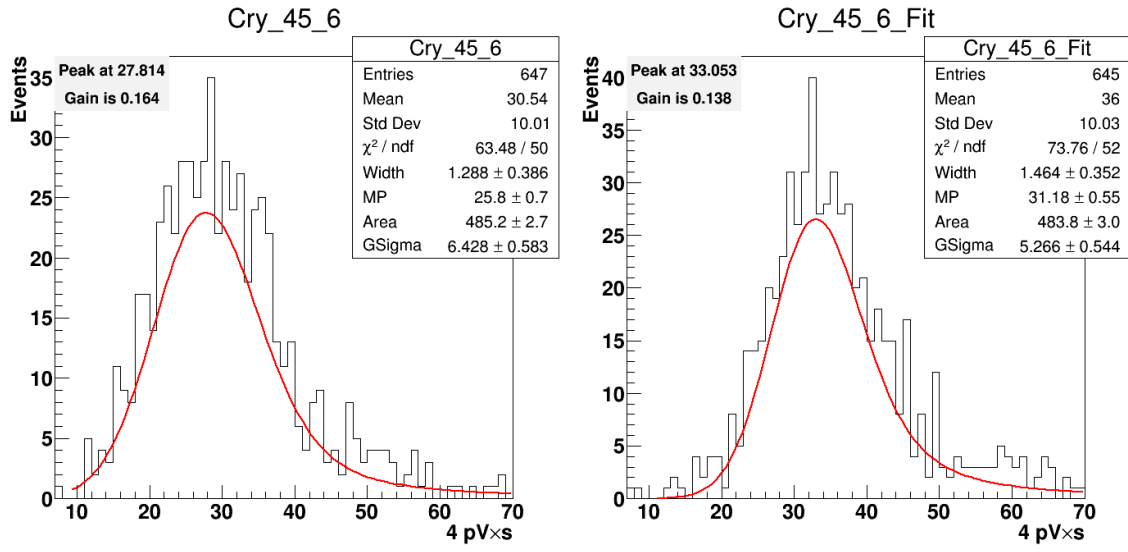


Figure 8: A comparison of the pulse-integral distribution and fit for integration with (right) and without (left) pulse-fitting, for the same crystal. In this case, the pulse-fitting did not substantially improve the distribution.

- [2] Holly Szumila-Vance. HPS Energy Calibration for the Spring 2015 Engineering Run, 6/8/16.
- [3] Andrea Celentano and Gabriel Charles. Characterization of the ecal crystal light yield and amplification chain, 8/19/14.
- [4] Nathan Baltzell. ECal Pulse Fitting, 9/9/15.